Int J Adv Manuf Technol (2016) 86:925–933
DOI 10.1007/s00170-015-8228-2

ORIGINAL ARTICLE

Arc characteristics and metal transfer modes in arcing-wire gas tungsten arc welding

Haichao Wang [1,2] · Shengsun Hu [1,2] · Zhijiang Wang [1,2] · Qifeng Xu [1,2]

Received: 8 July 2015 / Accepted: 10 December 2015 / Published online: 29 December 2015

Abstract Arcing-wire gas tungsten arc welding is an innovative process developed as a variant of gas tungsten arc welding to reinforce the deposition rate by utilizing bypass arc energy. After establishing an experimental platform, the experiments were conducted to study the arc characteristics, interaction of the main and bypass arcs, and metal transfer behavior. Magnetic arc blow, location of the bypass arc root, and shielding gas flow were found to cause arc deflection and an invisible obstacle between the arcs in arcing-wire gas tungsten arc welding. The bypass arc voltage should be controlled carefully to maintain the stability of the welding process. Globular transfer, short-circuiting transfer, and continuous bridging transfer could be obtained, which were determined by wire feed speed (the melting current) and the distance from the wire tip to the workpiece as well as the welding direction.

Keywords Magnetic arc blow · Metal transfer behavior · Arc characteristics · Deposition rate · Arcing-wire gas tungsten arc welding

1 Introduction

Gas tungsten arc welding (GTAW), for its stable arc process and high-quality products, has been successfully used in welding metal materials, especially in aluminum alloys, stainless steel, and the root pass welding on pipes and thick plates [1–3]. The process often requires filler metals for a desired deposition rate [4]. Cold-wire GTAW and hot-wire GTAW are currently the main processes used in industrial production. In hot-wire GTAW, the wire is preheated to 300–500 °C before the wire is fed into the weld pool, thus improving productivity and deposition rate. The deposition rate of hot-wire GTAW is double that of cold-wire GTAW.

Traditional hot-wire GTAW (Fig. 1a) and arc-assisted hot-wire GTAW (Fig. 1b) are two approaches that commonly use a preheated wire [5, 6]. The wire feeder is independent from the GTAW power source, and there is another preheating power source to apply current to the wire or to produce an arc between the auxiliary GTAW torch and wire. The filler wire, as shown in Fig. 1, remains in solid state before it is fed into the weld pool, although it is preheated. And, the wire needs more heat from the weld pool [4] to be melted and to be transferred into the weld pool. In other words, the welding current should be sufficiently large to maintain a large weld pool and to provide more energy to further melt the filler wire. Thus, the heat input of GTAW restricts the deposition rate in some ways.

Arcing-wire GTAW, which is a GTAW variation, is an innovative welding process inspired by the double-electrode arc welding process [6, 7]. The arcing-wire GTAW (Fig. 2b) process [4, 6], in which the bypass arc melts the wire directly, differs from traditional hot-wire GTAW (Fig. 2a) in the melting mode of filler wires. The significant difference is that traditional hot-wire GTAW utilizes resistive or auxiliary arc heat to preheat the wire, whereas arcing-wire GTAW uses bypass arc energy to melt the wire and transfers molten metal into the weld pool in the form of droplets. In arcing-wire GTAW, the wire feed speed corresponds with the melting current determined by the gas metal arc welding (GMAW) power source.

✉ Zhijiang Wang
wangzj@tju.edu.cn

[1] Tianjin Key Laboratory of Advanced Joining Technology, Tianjin University, 135 Yaguan Road, Jinnan District, Tianjin 300350, China

[2] School of Materials Science and Engineering, Tianjin University, Tianjin 300350, China

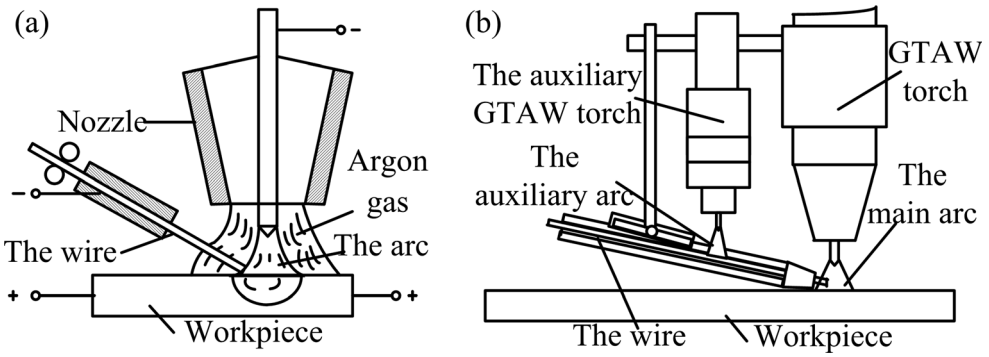

Fig. 1 Hot-wire GTAW: **a** traditional hot-wire GTAW and **b** arc-assisted hot-wire GTAW [5, 6]

The dependencies of weld stability, spatter generation, and welding defects on the dynamic behavior of the welding process necessitate deep understanding of the welding process [7, 8]. Therefore, to understand the mechanism of the coupled arc in arcing-wire GTAW, this study examines the arc characteristics, interaction of the two arcs, and the metal transfer behavior in arcing-wire GTAW by using a high-speed camera.

2 Arcing-wire GTAW system

The arcing-wire GTAW system is composed of two power sources, a GTAW power source running in constant current (CC) mode and a GMAW power source running in constant voltage (CV) mode [4, 9, 10]. Figure 3 illustrates the arcing-wire GTAW system, in which two torches are integrated and the following two arcs are established: the main arc (V_1) supplied by the CC power source is established between tungsten electrode (cathode) and workpiece (anode), while the bypass arc (V_2) supplied by the CV power source is established between the filler wire (anode) and the tungsten electrode (cathode). The voltage of the bypass arc supplied by the GMAW power source is an important adjustable parameter in the arcing-wire GTAW process. The bypass arc voltage should be 2–4 V higher than the main arc voltage to ensure that the bypass arc can be ignited.

In arcing-wire GTAW, the wire tip is mainly heated by the heat at the anode region of the bypass arc and the resistance heat. The heat provided by arcing-wire GTAW to melt the wire is about

$$k = I_{\mathrm{GMAW}} \frac{V_{\mathrm{GMAW}} + V_{\mathrm{anode}}}{V_{\mathrm{GMAW}}} \quad (1)$$

times that provided by hot-wire GTAW [4]. In Eq. (1), V_{GMAW}, I_{GMAW}, and V_{anode} are the wire voltage, melting current, and the anode voltage fall of the bypass arc in arcing-wire GTAW. Thus, the energy for melting the wire provided by arcing-wire GTAW is theoretically larger than that provided by traditional hot-wire GTAW.

3 Experiment design

Arcing-wire GTAW was performed on a carbon steel plate. Figure 4 illustrates the geometrical relationship between the integrated torches and workpiece [10, 11]. The distances d_1 and d_2 were set at 5 and 8 mm, respectively, and d_3 was determined by the bypass arc voltage. The torch angle between the GTAW and GMAW torches was maintained constant at 45° (θ). To avoid gas disturbance from influencing the stability of the integrated arc and to protect the tungsten electrode from overburning, only the tungsten electrode was shielded in argon gas (Ar with a purity of 99.99 %). The wire extended to the nozzle of the GTAW torch, but no shielding gas was supplied for GMAW.

Two Hall sensors, as shown in Fig. 3, were used for detecting current waveforms for the GTAW and GMAW. A high-speed camera, equipped with a 940-nm filter and operating at 500 frames per second (fps), was installed perpendicular to the plane determined by the welding direction and integrated torches.

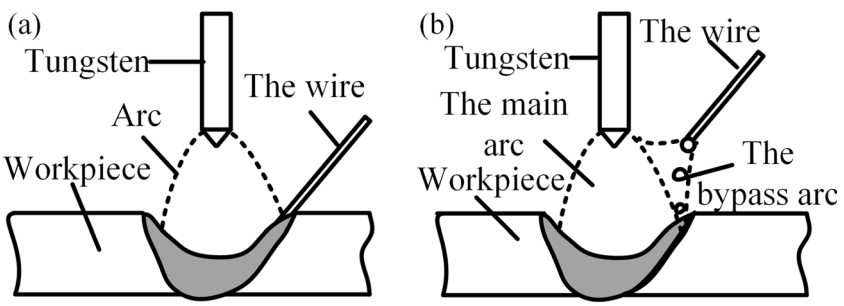

Fig. 2 Comparison of **a** hot-wire GTAW with **b** arcing-wire GTAW [4, 6]

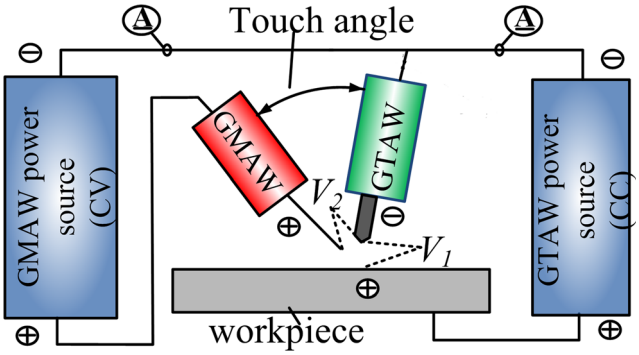

Fig. 3 Schematic diagram of the arcing-wire GTAW system

In the experiments, the main arc started first and the bypass arc followed closely. The GMAW torch was leading, and the GTAW followed behind in experimental group 1 and group 2. The high-speed camera and the data acquisition system started to work once the process became stable. The experiments were divided into two groups. Group 1 experiments examined the influence of the bypass arc voltage on the welding process stability at a given constant wire feed speed (*WFS*) of 2.1 m · min^{-1}. Three values of arc voltage were assigned to the bypass arc to explore the most appropriate voltage supplied by the GMAW power source, which will be used in group 2. The parameters of the group 1 experiments are shown in Table 1.

The mechanisms of the arc characteristics and metal transfer modes in arcing-wire GTAW for different *WFS* (I_{GMAW}) values were studied in the group 2 experiments. Table 2 shows the parameters of the group 2 experiments.

Another experiment (experiment 6) was conducted with the same welding parameters as experiment 4 but with a different welding direction. Experiment 6 aimed at studying the weld shaping in different welding directions and the influence of the main arc length on the metal transfer modes.

4 Experimental results and discussion

As d_1 and main arc current (I_{GTAW}) were set as constant, the main arc voltage (V_1) and I_{GTAW} were kept similar for all the experiments designed in Sect. 3, where I_{GTAW} fluctuates around 120 A and V_1 fluctuates around 11 V. Figure 5 gives the typical main arc voltage and current waveforms, which were obtained in experiment 1.

Table 1 Parameters of group 1 experiments

Parameters	Experiment 1	Experiment 2	Experiment 3
d_1 (mm)	6	6	6
V_2 (V)	14	19	23.5
Main arc current (A)	120	120	120
WFS (m · min^{-1})	2.1	2.1	2.1
Welding speed (mm · s^{-1})	1.5	1.5	1.5
Shielding gas (L · min^{-1})	15	15	15

4.1 Typical coupled arc for arcing-wire GTAW

The typical coupled arc in arcing-wire GTAW, illustrated in Fig. 6a, shows that the coupled arc was split into two parts, the main arc and the bypass arc. The main arc was identical to the bell-shaped arc of GTAW, except that it deflected slightly away from the centerline of the GTAW torch, whereas the deflection of the bypass arc was larger than that of the main arc. The root of the bypass arc, unlike that of the traditional GMAW arc, was lamellar and surrounded one side of the droplet, and the arc root area wandered with increasing droplets. There appeared an invisible obstacle between the two arcs.

Figure 6b shows the magnetic field distribution diagram, the ampere force direction of the bypass arc (F_2') under the magnetic field environment caused by the main arc current, and that of the main arc (F_1') under the magnetic field caused by the melting current. The thin arrow in red shows the direction of the melting current I_{GMAW}, while the thin arrow in blue shows the direction of the GTAW current I_{GTAW}. As the currents through the two arcs are opposite to each other, they repel each other because of the ampere forces F_1' and F_2', which explain the deflections of the arcs. As the bypass arc is established between the two electrodes and the melting current (I_{GMAW}) merges into the GTAW torch, the current in the

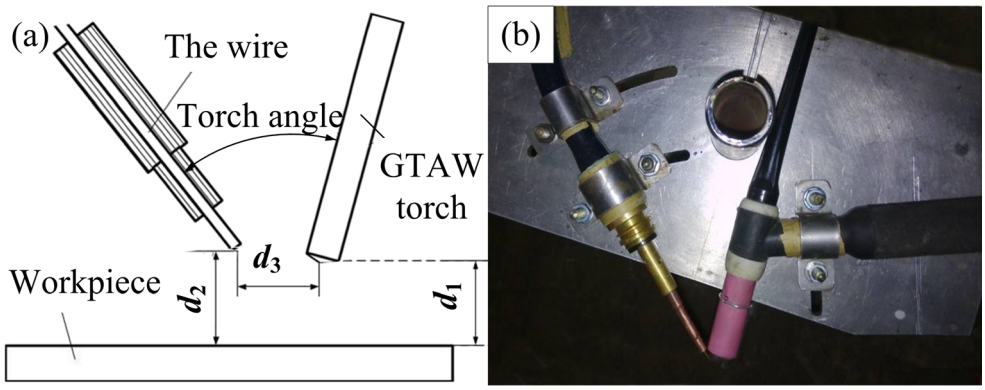

Fig. 4 Integrated torches: **a** geometrical relationship between the integrated torches and workpiece [10, 11] and **b** the picture of the integrated torches

Table 2 Parameters of group 2 experiments

Parameters	Experiment 4	Experiment 5
d_1 (mm)	6	6
Main arc current (A)	120	120
WFS ($m \cdot min^{-1}$)	2.3	2.8
Welding speed ($mm \cdot s^{-1}$)	1.5	1.5
Shielding gas ($L \cdot min^{-1}$)	15	15

GTAW torch is larger than I_{GTAW}. Therefore, the magnetic field around the GTAW torch is stronger than that around the GMAW torch, which makes the bypass arc deflect more than the main arc.

As mentioned above, the tungsten electrode was shielded in argon gas (99.99 % Ar) but no shielding gas was supplied for the GMAW torch. Therefore, the shielding gas blew the droplet away and an invisible obstacle (a "cold gas layer" which has a lower temperature than the arc) was established between the two arcs. The gas flow made the bypass arc deflect more than the main arc. The direction of the gas flow is not the same as that of the ionized particles in the arc, which will blow away some ionized particles. The lesser number of ionized particles make the arc temperature low (which is indicated by the low brightness in Fig. 6a and looks like an obstacle between the two arcs) or even worse extinguish the bypass arc.

The root of the bypass arc is located at one side of the droplet. This side of the bypass arc is near the main arc, and it could be heated to a higher temperature so that the arc is established easily. The bypass arc was further repelled toward the other side because of the electromagnetic force and the reverse force of the molten metal evaporation on the droplet surface. In this case, it is difficult for the droplet to approach the main arc. The forces acting on the droplet are different from those acting on the droplet in the GMAW process. They influence the metal transfer modes, which will be discussed later.

4.2 Influence of bypass arc voltage

The arc images of experiments 1, 2, and 3 recorded by the high-speed camera are shown in Fig. 7a–c, respectively. The moments for each image are marked in the images, as revealed in Fig. 7. The bypass arc in experiment 1 stayed uniform during the entire process, while those in experiments 2 and 3 were intermittent. This shows that the variable bypass arc voltage (V_2) influences the discontinuity of the bypass arc. Similar to the traditional GMAW welding process, the distance between the wire and GTAW torch (d_3) changes with increasing V_2. The larger the V_2 is, the longer the d_3 is. Longer d_3 makes it difficult for the ionized particles to pass through the bypass arc, and the shielding gas flow will make it more difficult. When V_2 is beyond the upper limit, d_3 is so long that the bypass arc extinguishes.

Figure 8 shows the melting current waveforms for the group 1 experiments. The current signal in experiment 1 (Fig. 8a) was continuous, but the other two current waveforms (Fig. 8c, e) were intermittent. The discontinuities appearing in the melting current waveforms for experiments 2 and 3 agree with the arc images in Fig. 7. Furthermore, the discontinuous time increased with the increasing bypass voltage.

The weld appearances of experiments 1 and 2 (Fig. 8b, d) were continuous. Their surfaces clearly showed overlapping traces of the droplets, which indicate that the droplet transfer mode is applicable only to slow-speed welding. In contrast, the weld appearance in experiment 3 (Fig. 8f) was discontinuous. All weld appearances agree with the melting currents in Fig. 8.

From the welding process analysis, the most stable arc in the group 1 experiments was with an arc voltage of 14 V, which was used in the group 2 experiments.

4.3 Results and analysis of the group 2 experiments

Arc images of experiments 4 and 5 are shown in Fig. 9c, f, respectively.

The metal transfer in experiment 4 (Fig. 9c) was in the globular transfer mode, which is a free flight transfer, and the droplet grew up to five to six times of the filler wire diameter before it dropped off owing to the low wire feed speed and low melting current. As shown in Fig. 6a, the forces exerted on the droplet F_1, F_2, F_3, and F_4 are the droplet gravity, the ampere force (caused by F_2' shown in Fig. 6b), the arc root repulsion of the bypass arc, and the surface tension,

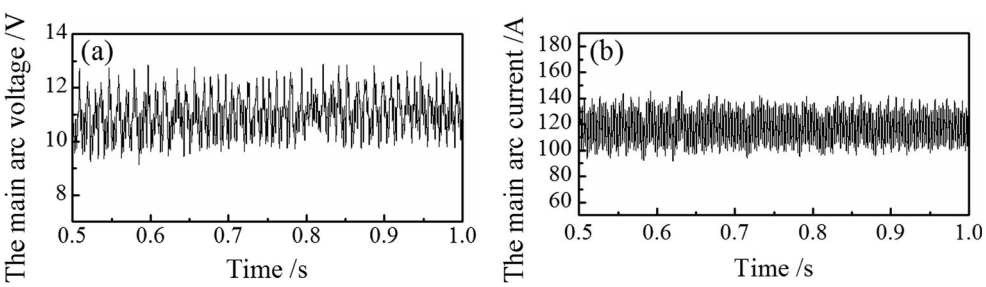

Fig. 5 Main arc voltage (**a**) and current (**b**) in experiment 1 processed by low-pass fast Fourier transform filtering

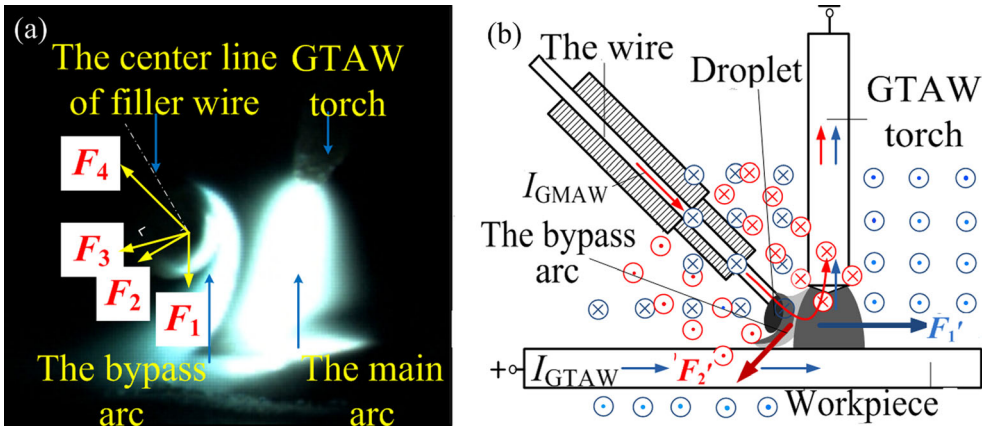

Fig. 6 Typical arc in arcing-wire GTAW: **a** arc in arcing-wire GTAW and the forces exerted on the droplet and **b** magnetic field distribution, the forces, and current direction in the arcing-wire GTAW system

respectively, in arcing-wire GTAW. As can be seen in Fig. 6a, the surface tension (F_4) is an oblique upward force since the droplet is heated on one side, which changes the direction of the surface tension. The surface tension hinders the metal transfer, but its effects were reduced due to the change in direction. The forces promoting the droplet dropping off (except for gravity) in the GMAW process, such as the electromagnetic force (at a higher melting current), the push force from the shielding gas, and the plasma jet force [12], have little effect on promoting the metal transfer. The electromagnetic force has a negligible pinch effect as the bypass arc root is located on one side of the droplet. Moreover, the plasma jet force, mainly caused by electromagnetic force, has a negligible effect too. Therefore, gravity F_1 becomes the most important force to promote the metal transfer with the help of the arc root repulsion force F_3. When d_2 is long enough in the arcing-wire GTAW process, the droplet will drop off only if gravity is greater than the vertical force of the surface tension, and that is why the droplet usually grows to a large size at a low melting current. In addition, the location where the droplets merged into the molten pool slightly deviated from the integrated arc area owing to the influence of F_2 and F_3. The transfer frequency is so low (about 0.5 Hz) that a discontinuous welding bead would occur easily if the welding speed was set inappropriately.

In experiments 1 and 4, the transfer frequency of the droplet increased from 0.3 to 0.5 Hz when the melting current increased from 35 to 45 A. The larger melting current increases F_2 and F_3. With increment of the melting current, the metal transfer frequency increases in arcing-wire GTAW.

With increment of *WFS*/the melting current to a high level, a special transfer mode—continuous bridging transfer—appeared as shown in Fig. 9f. The filler wire would plug into the weld pool, and the bypass arc disappeared. The bypass arc voltage and melting current were continuous as shown in Fig. 9d, e. The existence of the melting current indicated a circuit looped by the melting current passing through the liquid bridge and the main arc.

For the bridging transfer mode in arcing-wire GTAW, the wire is preheated as in traditional hot-wire GTAW using resistance heat. In traditional hot-wire GTAW, the wire tip is preheated by resistance heat at a thermal power of

$$P'_{w} = I'^{2}_{GMAW} R_{w} = V'_{GMAW} I'_{GMAW} \quad (2)$$

And the arc energy (P'_{arc}) is determined by

$$P'_{arc} = V'_{GTAW} I'_{GTAW} \quad (3)$$

Here, V'_{GMAW}, I'_{GMAW}, R_w, V'_{GTAW}, and I'_{GTAW} are the wire voltage, hot-wire current, wire resistance, arc voltage, and

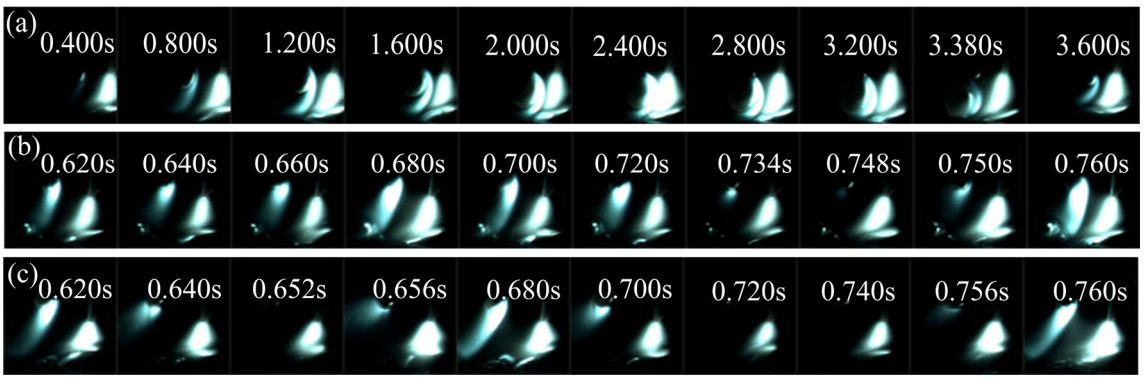

Fig. 7 Arc profiles of group 1 experiments: **a** experiment 1, **b** experiment 2, and **c** experiment 3

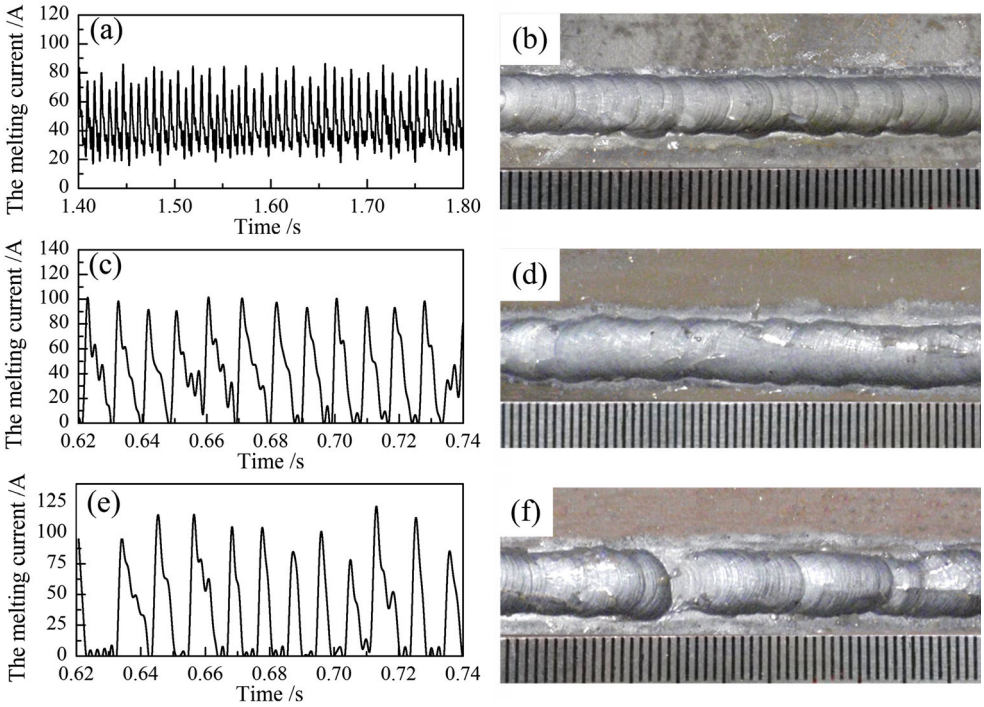

Fig. 8 Melting current waveforms processed by low-pass fast Fourier filtering and weld appearances in group 1 experiments: **a**, **b** for experiment 1, **c**, **d** for experiment 2, and **e**, **f** for experiment 3

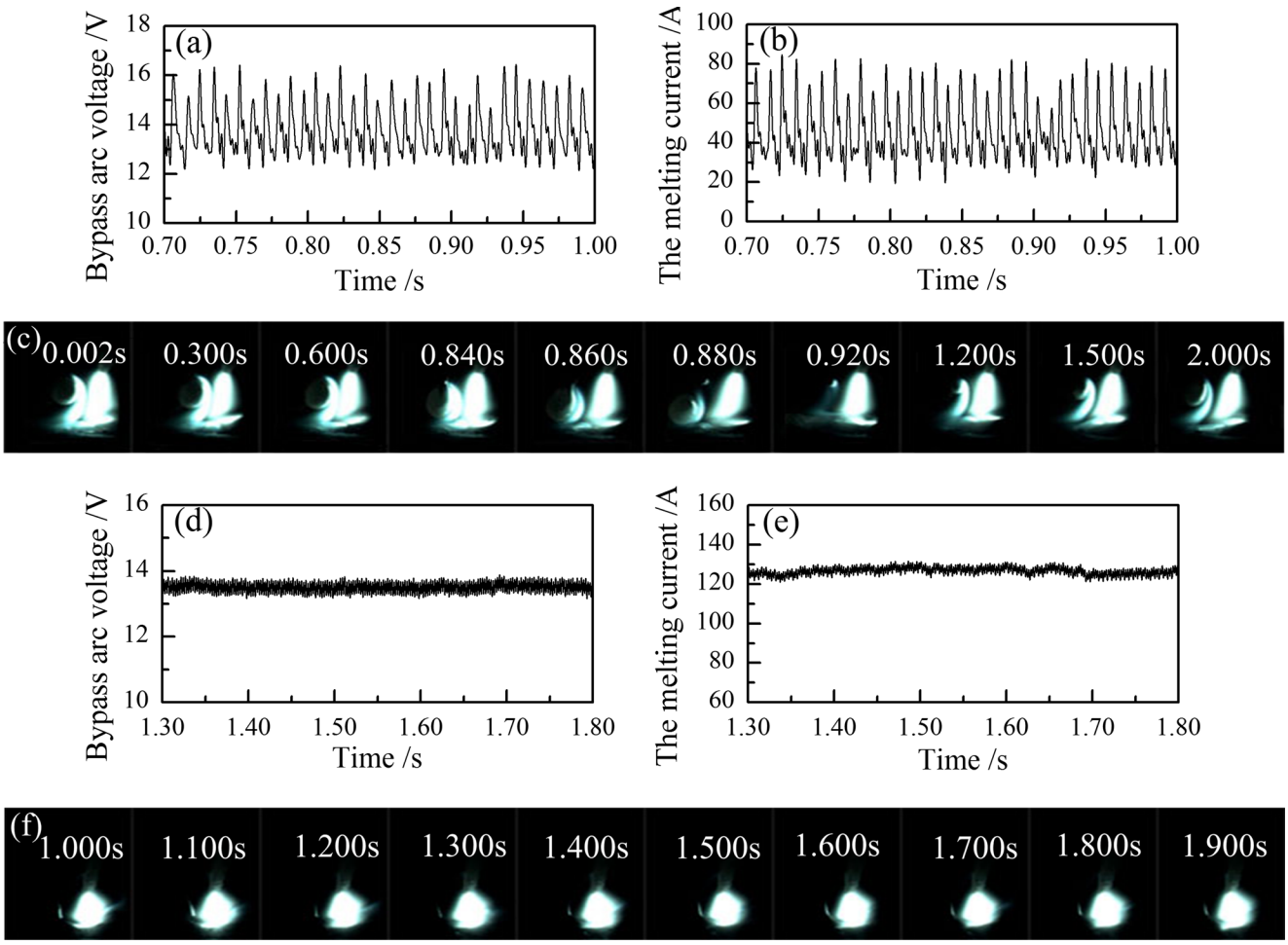

Fig. 9 Bypass arc voltage, melting current waveform processed by fast Fourier transform filtering, and arc images of experiment 4 (**a**–**c**) and those of experiment 5 (**d**–**f**)

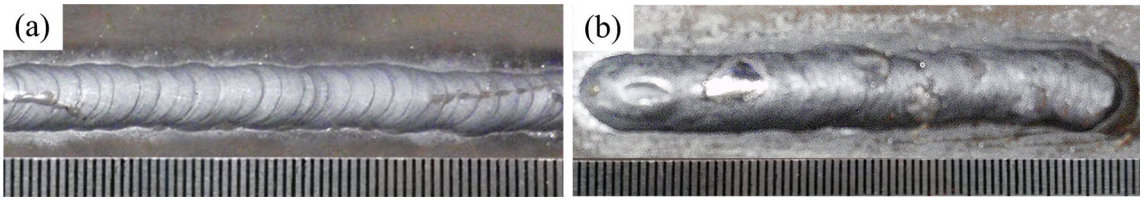

Fig. 10 Weld appearances of experiments 4 (**a**) and 5 (**b**)

welding current, respectively, in traditional hot-wire GTAW. The wire heating power and arc energy in the arcing-wire GTAW of experiment 5 are

$$P_{\mathrm{w}} = I_{\mathrm{GMAW}}^{2} R_{\mathrm{w}} \tag{4}$$

and

$$P_{\mathrm{arc}} = V'_{\mathrm{GTAW}}\left(I_{\mathrm{GMAW}} + I'_{\mathrm{GTAW}}\right) \tag{5}$$

respectively, where I_{GMAW} is the melting current in arcing-wire GTAW as mentioned above. Arc energy of arcing-wire GTAW is about

$$k = \frac{P_{\mathrm{arc}}}{P'_{\mathrm{arc}}} = 1 + \frac{I_{\mathrm{GMAW}}}{I'_{\mathrm{GTAW}}} \tag{6}$$

times that of traditional hot-wire GTAW.

In summary, the effect of the melting current, for the bridging transfer mode in arcing-wire GTAW, is equivalent to that of the increment of the weld pool caused by increasing the GTAW current in hot-wire GTAW. In traditional hot-wire GTAW, the hot-wire current (I'_{GMAW}) should be controlled carefully to maintain welding stability; otherwise, the bridging transfer mode will be destroyed. In arcing-wire GTAW, the current flowing through the filler wire (I_{GMAW}) is theoretically adjustable in a large range. The bridging transfer mode can even be maintained at a large melting current, greater than or comparable to the main arc current ($I'_{\mathrm{GMAW}} \leq I_{\mathrm{GMAW}}$, namely, $P'_{\mathrm{w}} \leq P_{\mathrm{w}}$), in which case the deposition rate will be improved.

Figure 10a, b exhibits the weld appearances of experiments 4 and 5. Overlapping traces of the droplets still appeared on the weld appearance in experiment 4, although the droplet transfer frequency increases as the melting current increases. The metal transfer frequency is still low in experiment 4. In contrast, the weld appearance in experiment 5 (Fig. 10b) formed well, where the deposition rate is apparently greater than that in experiment 4.

4.4 Influence of welding direction

Figure 11 shows that a short-circuiting transfer period occurred during the welding process in experiment 6. The figure presents the different results in comparison with the

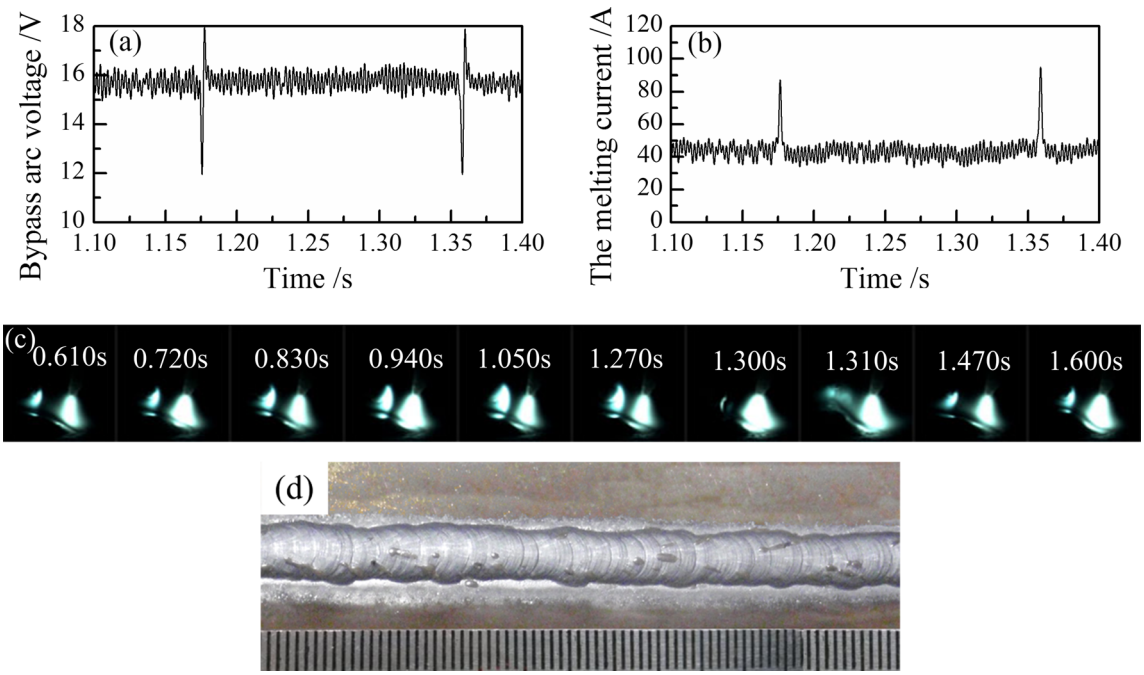

Fig. 11 Results of experiment 6: **a** the bypass arc voltage, **b** the melting current waveform (by low-pass fast Fourier transform filtering), **c** arc profiles, and **d** weld appearance

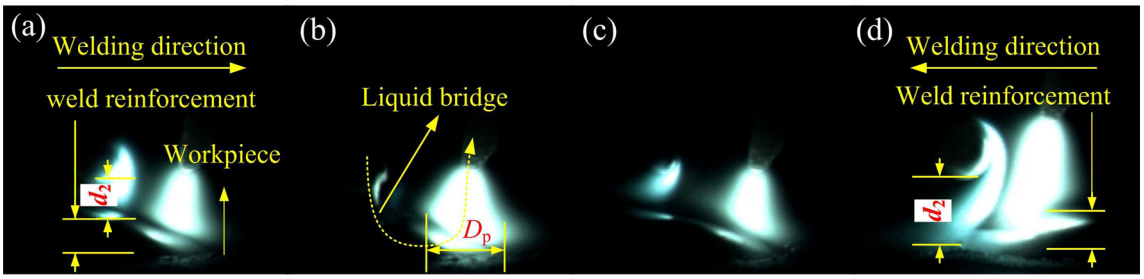

Fig. 12 Arc images at **a** the period before short circuiting, **b** short-circuiting period, and **c** the period after the droplet transfers in experiment 6 with a comparison with **d** an arc image of experiment 4

experiment 4 owing to the different welding directions. The arc in experiment 6 was similar to that in experiment 4 during the bypass arc duration, but at the moment of short circuiting, the bypass arc extinguished. The bypass arc voltage and melting current waveforms shown in Fig. 11a, b indicated that the melting current still existed when the droplet touched the workpiece. The melting current (dashed arrow in Fig. 12b) flew from a droplet bridge to the workpiece and passed through the main arc to the GTAW torch during the short circuiting, although the bypass arc disappeared. Figure 11d shows the weld appearance; it is continuous, but the weld bead is uneven.

In contrast to the arc before short circuiting (Fig. 12a) and that after droplet transfer (Fig. 12c), the main arc column diameter and arc diameter on the workpiece (D_p) increased when the droplet contacted the workpiece. The bypass arc ignited again with the wire approaching the main arc. The main arc shrunk to its original size, and a new period began.

The difference in transfer modes in experiments 4 and 6 is indeed caused by the different d_2 (Fig. 12a, d) for different welding directions. Weld reinforcement would decrease d_2 in experiment 6 (Fig. 12a), while in the other direction in experiment 4, d_2 was larger (Fig. 12d). If d_2 was lower than a threshold, the droplet would touch the workpiece before it dropped off from the wire tip, and the short-circuiting transfer occurred. Therefore, two transfer modes, free transfer and touching transfer, occurred in the arcing-wire system under the same parameters, except for the welding direction.

The stability of arc and metal transfer modes are also affected by the torch angle (θ), the relative position of the two torches, and the shielding gas flow rate.

5 Conclusions

An innovative welding process, arcing-wire GTAW, which involves melting the filler wire by utilizing bypass arc energy, was established. The arc behaviors and metal transfer modes in arcing-wire GTAW were investigated. It can be concluded that

1. The arc profile of arcing-wire GTAW can be divided into two parts, the main arc and the bypass arc. Magnetic arc blow, location of bypass arc root, and shielding gas flow mainly cause the deflection of the arcs and the invisible obstacle between the arcs.
2. The bypass arc voltage is the key factor influencing the welding process stability.
3. The melting current (I_{GMAW}) and the distance from the wire tip to the workpiece (d_2) determine the metal transfer modes. If I_{GMAW} is large and d_2 is large too, globular transfer occurs, and the transfer frequency will increase if I_{GMAW} increases. If I_{GMAW} is small and d_2 is small too, short-circuiting transfer will occur. If I_{GMAW} is large but d_2 is small, continuous bridging transfer can be obtained when I_{GMAW} and d_2 match well.
4. The bridging transfer mode, which is beneficial for improving arc stability, productivity, and deposition rate, would provide high-quality weld joints.

Acknowledgments This work is funded by the Innovation Fund of Tianjin University. We thank Dr. Li Huan for the assistance with high-speed imaging.

References

1. Moniz BJ, Miller RT (2010) Welding skill. American Technical Publisher
2. O'Brion RL (1991) Welding handbook. Welding Process. American Welding Society, Miami
3. Alexander CK, Sadiku MNO (2000) Fundamentals of electric circuits. McGraw Hill
4. Chen JS, Lu Y, Li XR, Zhang YM (2012) Gas tungsten arc welding using an arcing wire. Weld J 91:261s–269s
5. Lv SX, Tian XB, Wang HT, Yang SQ (2007) Arcing heating hot wire assisted arc welding technology for low resistance welding wire. Sci Technol Weld Join 12:431–435
6. Lu Y, Chen SJ, Shi Y, Li XR, Chen JS, Kvidahl L, Zhang YM (2014) Double-electrode arc welding process: principle, variants, control and developments. J Manuf Process 16:93–108
7. Kah P, Suoranta R, Martikainen J (2013) Advanced gas metal arc welding processes. Int J Adv Manuf Technol 67:655–674
8. Doodman Tipi AR, Hosseini sani SK, Pariz N (2015) Improving the dynamic metal transfer model of gas metal arc welding (GMAW) process. Int J Adv Manuf Technol 76:657–668

9. Li KH, Zhang YM (2010) Interval model control of consumable double-electrode gas metal arc welding process. IEEE Trans Autom Sci Eng 7:826–839
10. Li KH, Zhang YM (2007) Metal transfer in double-electrode gas metal arc welding. J Manuf Sci Eng 129:991–999
11. Li KH, Zhang YM, Xu P, Yang FQ (2008) High-strength steel welding with consumable double-electrode gas metal arc welding. Weld J 87:57–64
12. Zhang W, Hua XM, Liao W, Li F, Wang M (2014) Behavior of the plasma characteristic and droplet transfer in CO_2 laser–GMAW-P hybrid welding. Int J Adv Manuf Technol 72:935–942